PNAS RESEARCH ARTICLE | EARTH, ATMOSPHERIC, AND PLANETARY SCIENCES OPEN ACCESS

What we can learn about Mars from the magnetism of returned samples

Benjamin P. Weiss[a,1], Elias N. Mansbach[a], Clara Maurel[b], Courtney J. Sprain[c], Nicholas L. Swanson-Hysell[d], and Wyn Williams[e]

Edited by Harry McSween, The University of Tennessee Knoxville, Knoxville, TN; received May 17, 2024; accepted August 21, 2024

The Red Planet is a magnetic planet. The Martian crust contains strong magnetization from a core dynamo that likely was active during the Noachian period when the surface may have been habitable. The evolution of the dynamo may have played a central role in the evolution of the early atmosphere and the planet's transition to the current cold and dry state. However, the nature and history of the dynamo and crustal magnetization are poorly understood given the lack of well-preserved, oriented, ancient samples with geologic context available for laboratory study. Here, we describe how magnetic measurements of returned samples could transform our understanding of six key unknowns about Mars' planetary evolution and habitability. Such measurements could i) determine the history of the Martian dynamo field's intensity; ii) determine the history of the Martian dynamo field's direction; iii) test the hypothesis that Mars experienced plate tectonics or true polar wander; iv) constrain the thermal and aqueous alteration history of the samples; v) identify sources of Martian crustal magnetization and vi) characterize sedimentary and magmatic processes on Mars. We discuss how these goals can be achieved using future laboratory analyses of samples acquired by the Perseverance rover.

Martian dynamo | paleomagnetism | Mars sample return | polar wander | potential biosignatures

Significance

It is unknown how and why Mars transitioned from once being warm and wet to now cold and dry. A longstanding hypothesis is that an early thick atmosphere was lost due to the decline of a dynamo once generated in its churning metallic core. Here, we describe how future laboratory measurements of returned samples like those being collected by the Perseverance rover can test this idea by establishing the lifetime, intensity, and direction of the ancient magnetic field. These measurements can also constrain other key processes in Martian evolution including how the field was generated, the possibility of plate tectonics, the mineralogy of the crust, how water and lavas flowed on the surface, and even whether the samples preserve fossils.

Although Mars does not have an internally generated magnetic field today, the presence of strong magnetization in the Martian crust and in some Martian meteorites demonstrates that there was once a global magnetic field on Mars (1). This field was likely generated by the dynamo process, in which the mechanical energy of an advecting, conductive fluid in the planet's metallic interior inductively drives electrical currents that generate a large-scale field. The intensity, geometry, and lifetime of the dynamo field are poorly known but have major implications for the thermal and climatic evolution of Mars and the possibility that it was habitable.

There are two key reasons we know so little about the history of Martian magnetism. First, our magnetic records from in situ on Mars are mainly limited to orbital measurements of the present-day remanent magnetic field of the crust. Second, laboratory studies of Martian rocks are limited to meteorites, most of which likely postdate the end of the dynamo and all of which both lack geologic context and are unoriented relative to Martian geographic coordinates. The Mars sample return campaign (MSR) aims to fundamentally change this by returning up to ~30 absolutely oriented samples (2), mostly from bedrock and that include materials likely formed while there was a dynamo. Here, we discuss how paleomagnetic and rock magnetic studies of returned samples from Mars could transform our understanding of Martian geology and astrobiology by addressing at least six key science objectives (Fig. 1):

1. Determine the history of the Martian dynamo field's intensity.
2. Determine the history of the Martian dynamo field's direction.
3. Test the hypothesis that Mars experienced plate tectonics or true polar wander.
4. Constrain the thermal and aqueous alteration history of the samples.
5. Identify sources of Martian crustal magnetization.
6. Characterize sedimentary and magmatic processes on Mars.

These investigations were highlighted as key goals for MSR by the International MSR Objectives and Samples Team (their objectives 2.1D, 2.2A, 3C, 5A, and 5B) (3) and were presented in an earlier form by ref. 4. We begin by reviewing the history of magnetic studies of the Martian crust and meteorites. We then discuss key paleomagnetic and rock magnetic science objectives for returned sample analyses and their implications for sample quality criteria. We then review the samples collected thus far by the Perseverance rover at Jezero crater, Mars, and make recommendations for the rover's future sampling and exploration. We end by discussing the implications for curation of the samples on Earth.

Author affiliations: [a]Department of Earth, Atmospheric, and Planetary Sciences, Massachusetts Institute of Technology, Cambridge, MA 02139; [b]CNRS, Aix Marseille Université, Institut de Recherche Pour le Développement (IRD), Institut National de Recherche Pour L'Agriculture, L'Alimentation et L'Environnement (INRAE), Centre Européen de Recherche et D'Enseignement des Géosciences de L'Environnement (CEREGE), Aix-en-Provence 13545, France; [c]Department of Geological Sciences, University of Florida, Gainesville, FL 32611; [d]Department of Earth and Planetary Science, University of California, Berkeley, CA 94720; and [e]School of GeoSciences, University of Edinburgh, Edinburgh EH9 3FE, United Kingdom

Author contributions: B.P.W., N.L.S.-H., and W.W. performed research; and B.P.W., E.N.M., C.M., C.J.S., N.L.S.-H., and W.W. wrote the paper.

The authors declare no competing interest.

This article is a PNAS Direct Submission.

[1]To whom correspondence may be addressed. Email: bpweiss@mit.edu.

This article contains supporting information online at https://www.pnas.org/lookup/suppl/doi:10.1073/pnas.2404259121/-/DCSupplemental.

Published January 6, 2025.

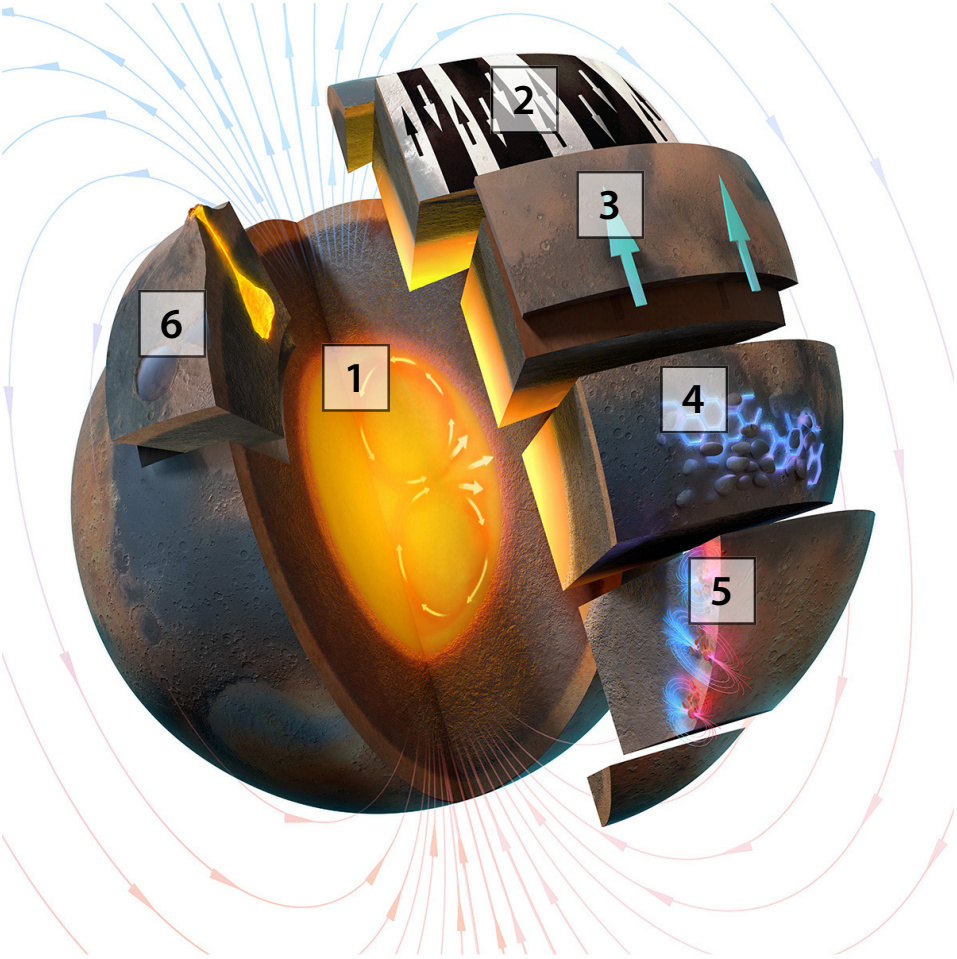

Fig. 1. Schematic showing six Mars magnetism science objectives. 1. Determine the history of the Martian dynamo field's intensity. 2. Determine the history of the Martian dynamo field's direction. 3. Test the hypothesis that Mars experienced plate tectonics or true polar wander. 4. Constrain the thermal and aqueous alteration history of the samples. 5. Identify sources of Martian crustal magnetization. 6. Characterize sedimentary and magmatic processes on Mars.

Introduction to Paleomagnetism and Rock Magnetism

The above science objectives center around future laboratory measurements of the i) remanent magnetization and ii) magnetic properties of Martian rocks. Remanent magnetization, the semipermanent alignment of electron spins within ferromagnetic minerals produced by exposure to magnetic fields, is a three-dimensional vector quantity, $\overrightarrow{M}$ (5). Remanent magnetization carried by geologic materials due to exposure to past natural magnetic fields is called natural remanent magnetization (NRM) (5). NRM can be acquired in many forms: as thermoremanent magnetization (TRM) when igneous and metamorphic rocks cool, as detrital remanent magnetization (DRM) when sedimentary rocks are deposited, or as crystallization remanent magnetization (CRM) when their constituent minerals crystallize. Long-term exposure to magnetic fields at low temperatures ($\lesssim$100 °C) can also produce a viscous remanent magnetization (VRM), while shock (>~5 GPa) in a field can instantaneously produce shock remanent magnetization (5). For weak fields, the NRM is

$$\overrightarrow{M} \sim X_r \vec{B}_{\text{paleo}}, \qquad [1]$$

where $\vec{B}_{\text{paleo}} = B_{\text{paleo}} \vec{b}_{\text{paleo}}$ is the ancient magnetizing field (with magnitude B_{paleo} and direction $\vec{b}_{\text{paleo}}$) and X_r is the remanence susceptibility, a sample-dependent constant (more generally, a second-rank tensor, $\boldsymbol{X}_\mathbf{r}$) quantifying the abundance and magnetization efficiency of the ferromagnetic grains (5). The study of NRM, which defines the discipline of paleomagnetism, provides powerful constraints on a diversity of past geologic processes acting on the nanometer to the planetary scale and has played a critical role in forming our modern understanding of Earth history, geophysics, and geobiology (6).

Eq. **1** shows that the magnitude of NRM reflects the intensity of past magnetic fields, B_{paleo}, as well as the ferromagnetic mineralogy, mineral abundances, and the form of NRM, all of which control X_r. The direction of NRM, $\vec{b}_{\text{paleo}}$, reflects the orientation of past magnetic fields relative to a sample. The NRM of a rock can be reset in the same ways it was originally acquired, including by reheating minerals above their Curie temperature (which ranges from 150 to 675 °C for typical Martian ferromagnetic minerals; see below) and/or during aqueous alteration and recrystallization.

Particularly powerful for paleomagnetic studies are field tests of stability, in particular conglomerate, fold, and unconformity tests (5, 7) (Fig. 2). These can establish whether NRM carried by rocks predates or postdates the formation of such structures. The NRM is judged to predate (postdate) such structures if NRM directions of a) conglomerate clasts are collectively random (uniform), b) rocks around a fold hinge cluster more (less) after correcting for bedding attitudes, and c) discontinuously (continuously) change across unconformities. This in turn constrains the temperature from ambient temperatures up to the Curie point and the timing of aqueous

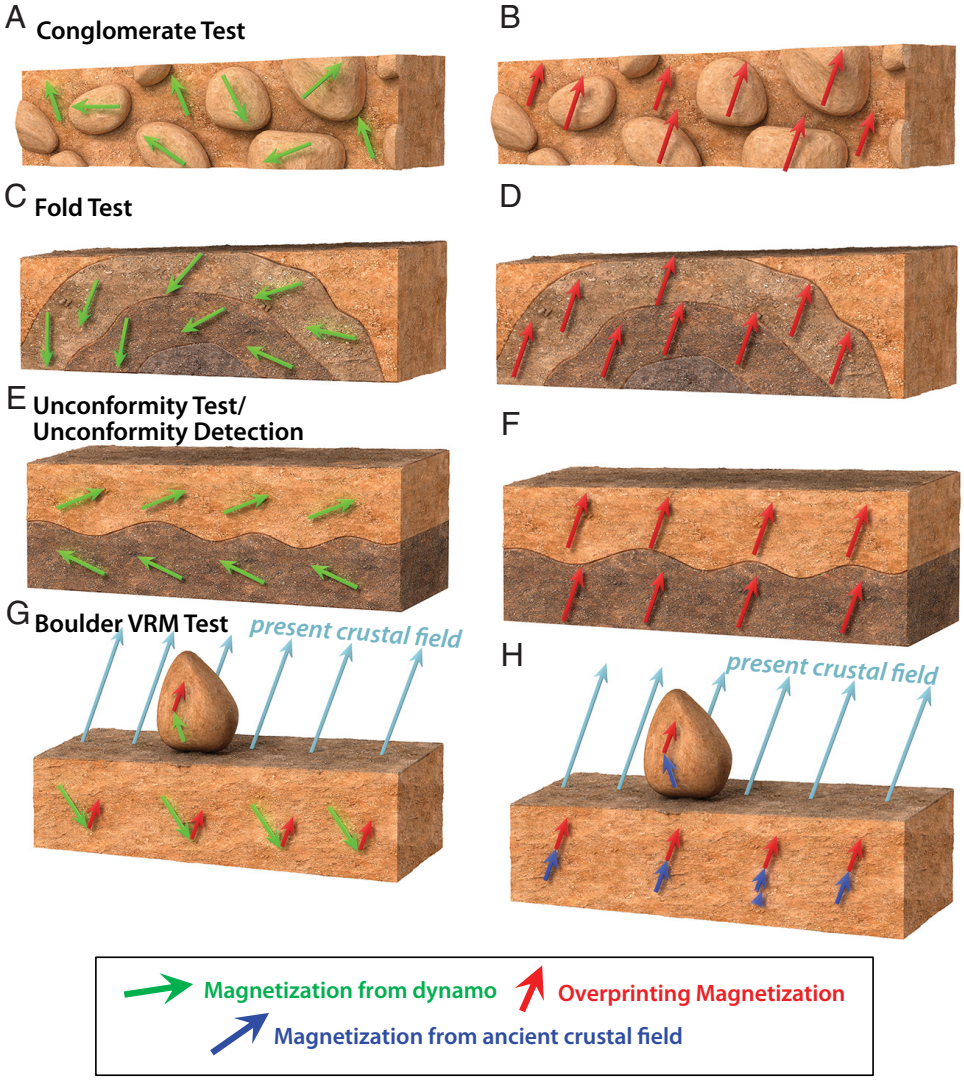

Fig. 2. Paleomagnetic field tests of stability. Shown are magnetization directions in a cross-section of bedrock containing dominantly magnetization formed in an ancient dynamo (red) versus younger overprints (*Right*). Green, blue, and red vectors denote magnetization produced by an ancient Martian dynamo, crustal field, or younger field of variable origin, respectively. Shown are vertical exposure outcrop faces and the overlying planetary surface. (*A* and *B*) Conglomerate test. Shown are boulders/lithic clasts (dark ovoids) and sedimentary/igneous matrix (lighter surrounding material). (*C* and *D*) Fold test. Lines trace bedding around a shallowly plunging anticlinal fold. (*E* and *F*) Unconformity test, or, alternatively, use of magnetization to identify a hidden unconformity. For the unconformity test, the curvy boundary between light and dark rocks denotes an unconformity confirmed by other data. For uniformity detection, sharp changes in magnetization direction can be used to identify a hidden unconformity (*Left*). (*G* and *H*) Boulder VRM test. (*Left*) Bedrock and boulder contain two-component magnetizations from ancient dynamo (TRM) and recent crustal field (VRM). (*Right*) Same as *Left* but ancient magnetization is TRM from crustal field with same orientation as crustal field today (blue arrows). Such a TRM would be difficult to identify from analyses of bedrock alone since it may have the same orientation as a VRM produced by the remanent field from this crustal TRM, whereas it could be identified from boulders for which they are differently oriented.

alteration relative to the deposition and deformation experienced by these rocks.

There are two key challenges for paleomagnetic studies of returned samples from Mars relative to those for Earth. First, Earth paleomagnetic studies, even those focused on a limited geographic location analogous to the region explored by the Perseverance rover, typically analyze an order of magnitude more samples than those planned for return by the MSR Campaign. The large number of Earth samples is usually driven by the need for multiple measurements from individual sites (e.g., time horizons) that collectively span an interval of 10,000 to 100,000 y, over which the time-averaged dynamo is indistinguishable from a planetocentric dipole aligned along the spin axis (8). Depending on the science objective, several to perhaps ~100 such sites typically need to be sampled for Earth; the equivalent number for Mars is unknown given our current lack of constraints on the Martian dynamo's time-variability. Second, paleomagnetic studies that seek to characterize the large-scale structure of Earth's dynamo (e.g., field geometry) and tectonics (e.g., differential plate motion associated with plate tectonics and rigid-body rotation of the mantle associated with true polar wander) sometimes need multiple sampling locations (each composed of multiple sites as described above) separated by thousands of km or more (9). However, the Perseverance rover is only expected to acquire samples over a geographic range spanning no more than a few tens of km.

Current Understanding of Martian Magnetism

Our current understanding of Martian magnetism is derived from two major datasets. First, we have in situ measurements of crustal magnetic fields from orbiters and landers and petrographic and magnetic observations of ferromagnetic grains from landers. Second, we have laboratory measurements of the paleomagnetism,

rock magnetic properties, and geochemistry of Martian meteorites. We discuss each in turn.

Spacecraft Data. In situ, geolocated measurements of the intensity and direction of the crustal magnetic field have been acquired by magnetometers on orbiters and landers (1, 10), while measurements of the mineralogy and magnetic properties of Martian materials have been acquired by magnet arrays, Mössbauer spectrometers, and X-ray diffractometers on landers (11, 12). Spacecraft magnetometry observations show that ancient regions of the southern hemisphere (with surface ages dominantly Early to Middle Noachian) are intensely magnetized (Fig. 3) with a vertically integrated intensity up to several orders of magnitude larger than that of Earth's oceanic crust (e.g., ref. 1). Downward continuation of field observations from altitude suggests that much of this region has surface fields of at least 1 to 10 μT (13). Weak, but nonzero, anomalies are also observed in the Pre-Noachian-aged Borealis basin in the northern hemisphere (1, 10) (Fig. 3). All of these fields are almost certainly produced by remanent magnetization that is the product of an ancient dynamo (1).

Because the formation of the Borealis basin would have thermally reset any preexisting remanent magnetization, these data hint that a dynamo was present at least in the Pre-Noachian (15). Nevertheless, it is possible that these anomalies were formed by crustal intrusions that occurred well after the pre-Noachian. Related to this, it is observed that Noachian and younger basins have significantly weaker crustal fields, which has been variably interpreted as indicating that the dynamo either ceased before (18), or initiated after (26), the end of the Noachian (1) (Fig. 3). An additional ambiguity is that nonuniformly oriented magnetization (e.g., like that produced by a time-varying dynamo) with spatial scales ≪150 km would be largely invisible from orbit, meaning that the absence of crustal fields does not require an absence of remanent magnetization (27, 28). Finally, spacecraft have detected magnetic anomalies above several Early Hesperian volcanic structures (15, 19, 20). Again, there is ambiguity about the relationship between ages from surface crater counts and magnetization timing, although this is less problematic for the relatively thin volcanic unit at Lucus Planum (15). In summary, spacecraft observations indicate that a dynamo existed on Mars, likely during at least the Pre-Noachian. However, the dynamo's intensity and lifetime are poorly constrained and the mechanisms that produced the strong magnetization in the crust are unknown (Fig. 3).

Crustal anomalies have also been used to determine crustal magnetization directions, which reflect the dynamo field's paleodirection. Assuming that the time-averaged Martian field had the geometry of a Mars-centric dipole pointing along the rotational axis (like for Earth) (6), the crustal remanent magnetization can be used to estimate the relative location of Mars's paleorotation pole at the time of magnetization. Analogous studies on Earth samples have provided

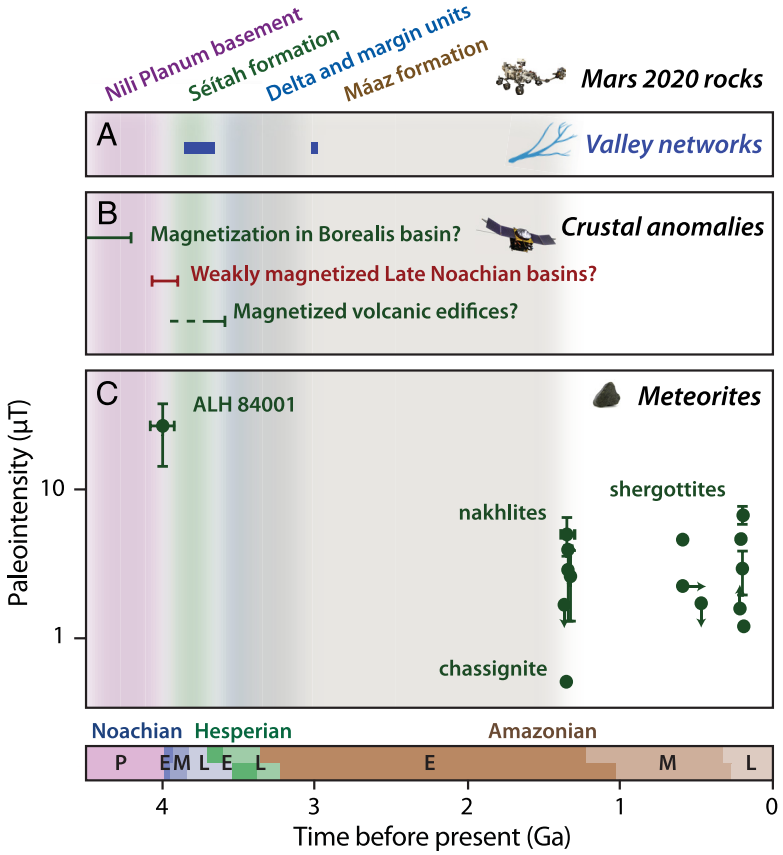

Fig. 3. History of the Martian dynamo and climate from meteorite and spacecraft data. (*A*) Timing of valley network fluvial activity (14). (*B*) Crustal anomaly constraints on the presence or absence of a dynamo (1). Weak but nonzero fields are present above the Pre-Noachian Borealis basin (15–17) (green). Near-zero fields are present above the Late Noachian basins (18) (red). Magnetic anomalies are also observed above volcanic structures with estimated ages as young as the Early Hesperian (15, 19, 20) (green). (*C*) Meteorite paleointensity estimates (*SI Appendix*, Table S1). Each green dot denotes paleointensity from studies of individual Martian meteorites. Circles represent actual paleointensities, circles with down and up arrows represent upper and lower paleointensity limits, and right and left arrows represent upper and lower limits on ages, respectively. Vertical shaded bars indicate estimated ages of rocks encountered by Mars 2020. Blue = western delta and crater margin units (21); brown = Máaz formation (22); green = Séítah formation (23); purple = Nili Planum basement (24). Stratigraphic relationships favor Máaz as older than the delta, which is contradicted by some crater counting age estimates. Chronology models shown in the *Bottom* panel are "Neukum system" (*Top*) and "Hartmann 2004 iteration" (*Bottom*) of ref. 25; P = Pre-, E = Early, M = Middle, and L = Late.

evidence for plate tectonics and true polar wander (9). Martian pole positions estimated in this way are scattered, but consistently deviate from the spin axis, which has been interpreted to indicate large-scale polar motion as well as a reversing dynamo (i.e., north and south poles flipping position) (e.g., ref. 1 and *SI Appendix*, Fig. S1).

A major limitation of spacecraft measurements is that the origin and mineralogy of the crustal sources of the anomalies are largely unknown given that the magnetization extends to depths of tens of km. Nevertheless, lander measurements show that some surface rocks contain abundant (up to >10 wt.%) ferromagnetic minerals with magnetite (Fe_3O_4) as likely the dominant mineral along with accessory hematite (Fe_2O_3), pyrrhotite ($Fe_{1-x}S_x$ for $x < 0.13$), and goethite (FeOOH) (e.g., refs. 12, 29, and 30).

Meteorite Measurements. Of the >150 known Martian meteorite pairing groups (31, 32), ~18 have had their paleomagnetism studied (*SI Appendix*, Table S1). The ages of the measured samples range from ~170 million years (Ma) to 4.1 billion years (Ga) ago, dating to the Amazonian, Noachian, and Pre-Noachian periods (31). Unlike spacecraft data, the original orientations and formation locations of Martian meteorites are largely unknown; as a result, only magnetization intensities and not absolute directions can be recovered. However petrographic and radioisotopic measurements powerfully constrain the mineralogical sources and ages of their magnetization records, while laboratory remagnetization analyses provide estimates of the field's paleointensity.

Martian meteorites contain the ferromagnetic minerals magnetite, titanomagnetite ($Fe_{3-x}Ti_xO_4$ for $x < 1$), and pyrrhotite (e.g., ref. 33). Most meteorites, including nearly all desert meteorites, have been substantially or completely remagnetized by collectors' hand magnets, such that they provide no constraints on the Martian paleofield (34). However, robust paleomagnetic records of the Martian field have been derived from at least one nakhlite and two shergottites, which demonstrate the presence of fields of ~2 to 5 μT on Mars at 192 ± 10 Ma, <574 Ma and 1,339 ± 8 Ma (*SI Appendix*, Table S1). Paleomagnetic studies of Martian meteorite Allan Hills (ALH) 84001 also estimated a high field strength of 28 ± 13 μT at 3.95 to 4.1 Ga, a time that overlaps with the estimate ages of some crustal anomalies (35, 36). Overall, Martian meteorites record the paleofield on Mars during at least four periods: 3.95 to 4.1 Ga, 1.3 to 1.4 Ga, 440 to 580 Ma, and 160 to 190 Ma (Fig. 3). It is unclear whether these estimates are a direct record of the dynamo or a crustal field (produced by an earlier dynamo). However, the order of magnitude drop in intensity between 3.9 and 1.3 Ga could be interpreted as a decline or even cessation of the dynamo during this interval.

If we assume the Martian crust carries a TRM acquired in a field of ~30 μT (e.g., paleointensity from ALH 84001), then all but ~5 measured meteorites have too low abundances of ferromagnetic minerals to account for the crustal magnetic anomalies (37, 38). Furthermore, all meteorites were likely ejected from the shallow crust (<1 km) (following ref. 31) and so may not be representative of the lithologies hosting the crustal anomalies in the deeper crust.

Limitations Relative to MSR. As discussed above, magnetic studies of the Martian crust and meteorites indicate that a dynamo was present on Mars, likely at least in the Pre-Noachian and possibly extending until at least the Early Hesperian. However, further progress from spacecraft datasets is highly limited relative to what can be expected from future laboratory measurements of returned samples. First, inferring magnetization distributions from a given set of crustal field measurements is a nonunique inverse problem (e.g., ref. 39). Second, remagnetization experiments cannot be conducted on the crust from orbiters, making it almost impossible to infer the paleointensity of the recorded field. Finally, crustal anomaly ages are poorly constrained because of the lack of radioisotopic measurements and the fact that crater counting of the surface may not constrain the timing of magnetization in the deep (tens of km) crust.

The Martian meteorite suite also has major limitations relative to returned samples. First, all but two known meteorite pairing groups are younger than 1.3 Ga (31). Furthermore, there are no samples from the Hesperian when Mars underwent a major change in climate and the dynamo may have declined (31). Second, many Martian meteorites were remagnetized by shock of up to tens of GPa during ejection, terrestrial weathering, and collector's hand magnets (40). Third, Martian meteorites are unoriented relative to Martian geographic coordinates (41). Fourth, their geologic context is largely unknown and there are no stratigraphically ordered sample sequences. Below, we show that all the deficits for both the crustal field and meteorite measurements would likely be addressed by the Perseverance rover sample suite.

Paleomagnetic and Rock Magnetic Science Objectives for Returned Samples

Future laboratory analyses of returned samples from Mars should address several major unsolved questions about the lifetime, history, and geometry of the dynamo, the history of planetary climate and habitability, the search for biosignatures of past life, and the thermal and tectonic evolution of the planet. Here, we discuss the aforementioned six key science objectives that could be achieved with MSR (Fig. 1).

Objective 1. Determine the History of the Martian Dynamo Field's Intensity. The present-day Martian atmosphere is sufficiently thin and cold such that liquid water is not stable on the surface. However, surface geomorphic evidence for the flow of liquids (14), the presence of crustal weathering minerals (42), and the enrichment of heavy isotopes of several atmospheric species (e.g., ref. 14) suggest that Mars had a several bar CO_2-rich atmosphere with surface temperatures possibly >273 K at least intermittently in the Hesperian period and earlier (14) (Fig. 3). A leading hypothesis for how this atmosphere was lost is that it was driven by nonthermal escape mechanisms (e.g., solar wind-induced sputtering and pickup) following the decline of an early strong (>~10 μT) global Martian magnetic field (43). Note, however, that a weak dynamo might enhance atmospheric loss relative to an unmagnetized planet (44).

Because of its possibly central role in Martian habitability, establishing the strength and lifetime of the dynamo is likely the most important question addressable by returned sample magnetic measurements (Fig. 1). As such, a key future test of the hypothesis that the dynamo decline was a causal factor in climate change is that it should have occurred prior to the onset of substantial atmospheric loss. Because the sustenance of a core dynamo requires vigorous advection of core fluids, determination of the lifetime and vigor of the dynamo also would constrain the thermal evolution of Mars' interior, which is in turn influenced by core crystallization (45) and plate tectonics (46). This objective can be achieved with laboratory measurements of the field intensity (B_{paleo} in Eq. **1**) from a suite of rocks of different ages ideally spanning at least the Pre-Noachian to the Early Hesperian. Measurements of the field direction ($\vec{b}_{paleo}$) from bedrock and float (e.g., boulders) would also be valuable for establishing the source of the magnetization. In particular, comparison of any VRM overprints on boulders and bedrock (acquired from prolonged exposure to the crustal field) could be used to test whether the non-VRM part of magnetization in bedrock is from a dynamo (Fig. 2).

Objective 2. Determine the History of the Martian Dynamo Field's Direction. Nearly all measurements of planetary samples other than those from Earth have only measured the paleofield intensity (41). MSR offers the opportunity of absolutely oriented paleodirectional measurements on Mars. Such measurements could answer fundamental questions about the nature of Mars's dynamo (Fig. 1). First, the mean paleofield direction and its time-variability may constrain the dynamo process and planetary heat flow regime. Convective dynamos in planets with relatively low core heat fluxes, high rotation rates, and small inner cores tend to be dipolar and aligned along the spin axis, whereas dynamos at the other extrema tend to be multipolar (47). It has been variably predicted that the Martian field would be largely dipolar like the Earth's or instead nondipole dominated (1). Time-resolved observations of magnetic reversals (Fig. 2*E*) could constrain the vigor of core convection and the intensity and spatial dependence of the core–mantle boundary heat flux (48). Furthermore, the identification of zones of opposite polarity could allow stratigraphy to be correlated over multiple, discontinuous sections. Such data, in combination with radioisotopic ages, would initiate the development of a geomagnetic polarity timescale (6) for Mars. As on Earth (6), stratigraphically bound reversal sequences could potentially be used as a relative dating tool for rocks. Laboratory analyses for this objective involve measurements of the absolute direction, $\vec{b}_{\text{paleo}}$.

Objective 3. Test the Hypothesis That Mars Experienced Plate Tectonics or True Polar Wander. Geologic and geophysical data have been tentatively interpreted to indicate that Mars has experienced plate tectonics (49, 50) and/or true polar wander (51) (Fig. 1). Independent evidence for true polar wander is provided by the equatorial position of the Tharsis volcanic province, whose emplacement may have rotated the mantle and crust by ~20° (52) and possibly also the offset of ice-rich polar deposits from the present-day spin axis by up to ~9° (53). The timing and magnitudes of these true polar wander events are poorly constrained, with estimates for the Tharsis event ranging from the Noachian to at least the Late Hesperian (52). Assuming an axial dipole geometry could be established for the time-averaged field (*Objective 2*), these hypotheses could be tested by estimating the locations of paleomagnetic poles (e.g., ref. 54) from paleomagnetic measurements of returned samples (*SI Appendix*, Fig. S1). In addition to their implications for formation time of Tharsis and ice-rich deposits, such measurements would potentially have at least two additional major implications. First, they could determine the paleolatitude of Jezero at the times when water flowed into the crater and when its rocks were aqueously altered. This would in turn constrain global paleoclimate models and their relationship with Mars' obliquity variations (14). Second, understanding the history of Martian true polar wander is also important for establishing whether an ocean existed in the Martian northern hemisphere (55) and the timing of the formation of Tharsis. This objective could be partly achieved using time sequences of progressive changes in $\vec{b}_{\text{paleo}}$ ideally over 100 Ma or more, assuming secular variation could be averaged (*Objective 2*). However, it will likely be difficult to use samples from a limited geographic location like that to be explored by the Perseverance rover to distinguish between plate tectonics versus true polar wander as the source of any interpreted tectonic motion.

Objective 4. Constrain the Thermal and Aqueous Alteration History of the Samples. Perhaps the most important objective of MSR is to search for fossils of past Martian life (3). Determining whether a sample contains potential biosignatures (e.g., microfossils and organic matter) and, if so, how, and when they formed (taphonomy) requires an understanding of the formation and subsequent alteration history of the rock host. This includes the history of diagenesis, weathering and aqueous alteration, oxidation and reduction, as well as thermal metamorphism and shock. Constraining the effects of such processes on the samples is also critical for achieving the other five MSR magnetic objectives, which rely on an understanding of the timing and form of NRM. These processes can be powerfully constrained using paleomagnetic field tests (Fig. 2) and measurements of mineral magnetic properties like Curie temperature and coercivity (resistance to being remagnetized by fields) (5). Laboratory analyses for this objective would involve measuring the relative direction of $\overrightarrow{M}$ and conducting a diversity of rock magnetic experiments.

Objective 5. Identify Sources of Martian Crustal Magnetization. Martian crustal magnetic fields today are the most intense known among planetary bodies, approaching the surface dynamo field of the Earth in some locations. The reason for this is unknown but could have major implications for the intensity history of the dynamo possibility of deep aqueous alteration of the crust (56). Eq. **1** shows that such intense NRM can be explained by either a strong dynamo field (B_{paleo} ~ 10 times higher than that of Earth, or ~500 μT) and/or a high abundance of magnetic minerals (X_r ~ 10 times higher than that of Earth's crust). Either a high B_{paleo} or X_r would have major implications for Mars science. If the surface dynamo field were tens of μT or larger, it may have partly shielded the atmosphere from solar wind sputtering and pickup (*Objective 1*). Alternatively, a high X_r may be the manifestation of a CRM, possibly formed by widespread aqueous alteration of the crust (56, 57). This has important implications for the possibility of a deep paleobiosphere (*Objective 6*) (58). Furthermore, analogous surface aqueous alteration processes associated with the formation of magnetite-rich mudstones at Gale crater (12) may have also generated H_2 that transiently warmed the planet and served as an energy source for organisms (58, 59).

Laboratory paleointensity measurements of surface samples can determine the magnetization intensity M and the paleointensity of the field that produced this, B_{paleo}. Furthermore, rock magnetic and petrographic measurements could determine, at least for surface rocks, X_r and its relationship to the identity, grain size, grain shape, and abundance of ferromagnetic minerals. Furthermore, the intensity of the crustal field at the sampling site could be estimated from paleointensity experiments on VRM overprints identified from float rocks (Fig. 2).

Objective 6. Characterize Sedimentary and Magmatic Processes on Mars. A key goal of MSR is to understand the nature and evolution of habitable environments (3). This includes the duration and degree of continuity of lake and fluvial activity and the setting in which rocks were aqueously altered. In particular, a key unsolved problem is whether minerals like phyllosilicates and magnetite that were produced by water–rock interactions and that are observed widely in Noachian and Early Hesperian terranes largely formed in situ (i.e., authigenically) or are detritus derived from even older terranes (42). Conglomerate tests (Fig. 2) could establish this through a comparison of the magnetization of magnetite-bearing matrix and clasts. Unconformity tests (Fig. 2) could identify hiatuses and hidden unconformities (e.g., paraconformities) in sedimentary sequences. Measurements of magnetic anisotropy (e.g., tensor form of susceptibility, X_r) could constrain fluid flow directions (60). Rock magnetic analyses could constrain the redox history of the Jezero lake system (*Objective 4*) including even potentially

biological iron cycling (61). Measurements of a boulder's VRM could be used to date the last time the boulder was rotated (e.g., by flooding or wind erosion) (62). Finally, the paleolatitude of Jezero could be estimated as a function of time (*Objective 3*).

Another goal of MSR is to understand the history of planetary igneous differentiation and volcanism (3). Analogously with sediments, paleomagnetic measurements of volcanic rocks can identify hiatuses through unconformity tests (Fig. 2) and flow directions using magnetic anisotropy measurements (60). Conglomerate tests (Fig. 2) on volcaniclastic rocks can determine their emplacement temperatures (63). Measurements of the magnetization directions held by primary and secondary assemblages can establish whether aqueous alteration occurred contemporaneously with eruption or later.

Desired Returned Sample Quality Criteria. *Objectives 1 and 4* require measurements of the field strength, B_{paleo}. Accurate paleointensity measurements can currently only be acquired for rocks that contain TRM (5). Therefore, igneous rocks are high priority for these objectives. Unaltered sedimentary rocks, which may contain DRM, and aqueously altered igneous and sedimentary rocks, which can carry CRM, will provide less accurate paleointensity estimates but often with a record that is more time-continuous than that of TRM-bearing rocks (6). Samples should ideally show no petrographic evidence for shock (i.e., <5 GPa) unless targeted specifically for records that formed during an impact event.

Essential for *Objectives 2 and 3*, and important for all objectives, is the ability to measure the absolute direction of $\vec{b}_{\text{paleo}}$ in Martian geographic coordinates. To enable this, all cores should be absolutely oriented to better than 5° (see ref. 41). Also, nearly all cores should be sampled from bedrock. An exception is that it would be useful to sample a boulder to infer the local crustal field direction (*Objective 5*) or to infer the timing of transport (*Objective 6*).

To anchor the time of their magnetization acquisition, the deposition, crystallization, and/or aqueous alteration events experienced by the samples should be amenable to radioisotopic dating, ideally using chronometers with closure temperatures similar to the Curie temperatures of Martian ferromagnetic minerals. Required for *Objectives 1–3*, but highly beneficial to all activities, is the acquisition of time sequences of B_{paleo} and $\vec{b}_{\text{paleo}}$, achieved from two different kinds of sample suites. First and most important are samples acquired from a range of stratigraphic positions. Second, are samples that contain both primary ferromagnetic minerals and secondary minerals produced by aqueous alteration.

Mars 2020 and the MSR Campaign

MSR will provide an unprecedented opportunity to address outstanding questions in Martian magnetism. As currently envisioned, MSR consists of a sequence of spacecraft missions beginning with sampling on Mars with the Perseverance rover (in progress) followed by launch and transfer of the samples to Earth (2). Here, we describe how the samples already acquired by Perseverance will powerfully enable returned sample science analysis to address the six MSR magnetism science objectives. *SI Appendix, Text* makes recommendations for future sampling by the rover outside the crater that will further address these objectives.

Perseverance is exploring and sampling within Jezero crater, a ~45-km diameter, Early–Late Noachian crater situated in the Nili Planum region (64) (Fig. 4). The crater lies just outside what is inferred to be the transient cavity of the Early–Late Noachian Isidis basin (64). Although orbital observations have not detected interior magnetic anomalies in Isidis, this does not preclude the presence of substantial fine-scale magnetization (see above). The west side of Jezero hosts what is thought to be the remnants of a delta associated with a fluvio-lacustrine system of likely Early Hesperian-Early Amazonian age (21).

Deltaic rocks consist of variably aqueously altered sandstones and siltstones with basaltic lithic grains, sulfate-rich mudstones, and carbonate-rich lithologies (21). These are thought to unconformably overlie a volcanic crater floor composed of Middle-Late Noachian aqueously altered olivine-rich rocks (Séítah formation) and Late Hesperian-Early Amazonian basaltic rocks (Máaz formation). Possible multiple hiatuses of unknown duration have been identified between and within the crater floor and fan (21, 22). Under the assumption that the crater floor rocks formed as flat lava flows, they were apparently uplifted and tilted up to ~15° possibly due to the uplift of the Séítah formation (22). The surrounding Nili Planum region, which is the source of detrital grains that make up the Jezero fan (69), hosts a diversity of Pre-Noachian to Noachian rocks including variably aqueously altered layered and fractured basement rocks, a regional olivine-carbonate-rich unit, and megabreccia (1 to 100 m blocks) which may be the product of the Isidis impact (24).

Current Samples. At the time of writing, Perseverance has collected 21 rock cores (70–72) (Fig. 4). The first 14 cores consist of seven paired samples taken within 1-m of each other from the same lithology. All but two of the 21 cores were acquired from bedrock, with the remaining two (Montdenier and Montagnac cores) collected from a tilted boulder (41). All rock samples are oriented with respect to Martian geographic coordinates to better than 2.7° (3σ), making them the first suite of absolutely oriented, stratigraphically bound bedrock samples from another planet (41). Rock samples were acquired from both the Séítah (e.g., Salette and Coulettes cores) and Máaz (e.g., Montdenier and Montagnac cores) formations on the crater floor (73) and from clastic and precipitated sedimentary rocks with basaltic, sulfate-rich, and carbonate-rich compositions on the delta (74) and adjacent crater margin units. The clastic samples include a granule-pebble conglomerate, the Otis Peak core, and coarse sandstones that are variably cemented with sulfate, carbonate, and silica. None of the samples shows any clear evidence in rover data of being shocked or modified by impacts.

Rover observations indicate the rock samples contain Fe-, Cr-, and Ti- oxides with grain sizes extending from several mm down to <20 μm (75). Although the rover cannot measure the crystal structures of these grains, by analogy with previous observations of Martian materials (see above), many of these oxides are likely ferromagnetic (75). The observations suggest that all but one of these minerals in both the igneous and the sedimentary rocks are primary (i.e., detrital or igneous) with the remaining one having formed during later aqueous alteration. There is no clear evidence from the relatively low spatial resolution (>0.1 mm) rover observations of metamorphic or shock effects (Fig. 4*A*).

Crater counting suggests that collectively, the sampled units have age estimates ranging from ~1.4 to 3.9 Ga (Middle Noachian to Early Amazonian). These ages, which can be refined through radioisotopic geochronology on returned samples, make Jezero and Nili Planum rocks ideal for constraining the lifetime of the dynamo (*Objective 1*) (Fig. 3). Because the crater floor rocks should contain TRMs, they may enable accurate measurements of the paleointensity of the field. Séítah samples (e.g., the Salette and Coulettes cores) could provide records from the critical period of climate change and possible decline in the field, while detrital grains in the Otis Peak core may provide the oldest paleointensity records (Figs. 3 and 4*B*).

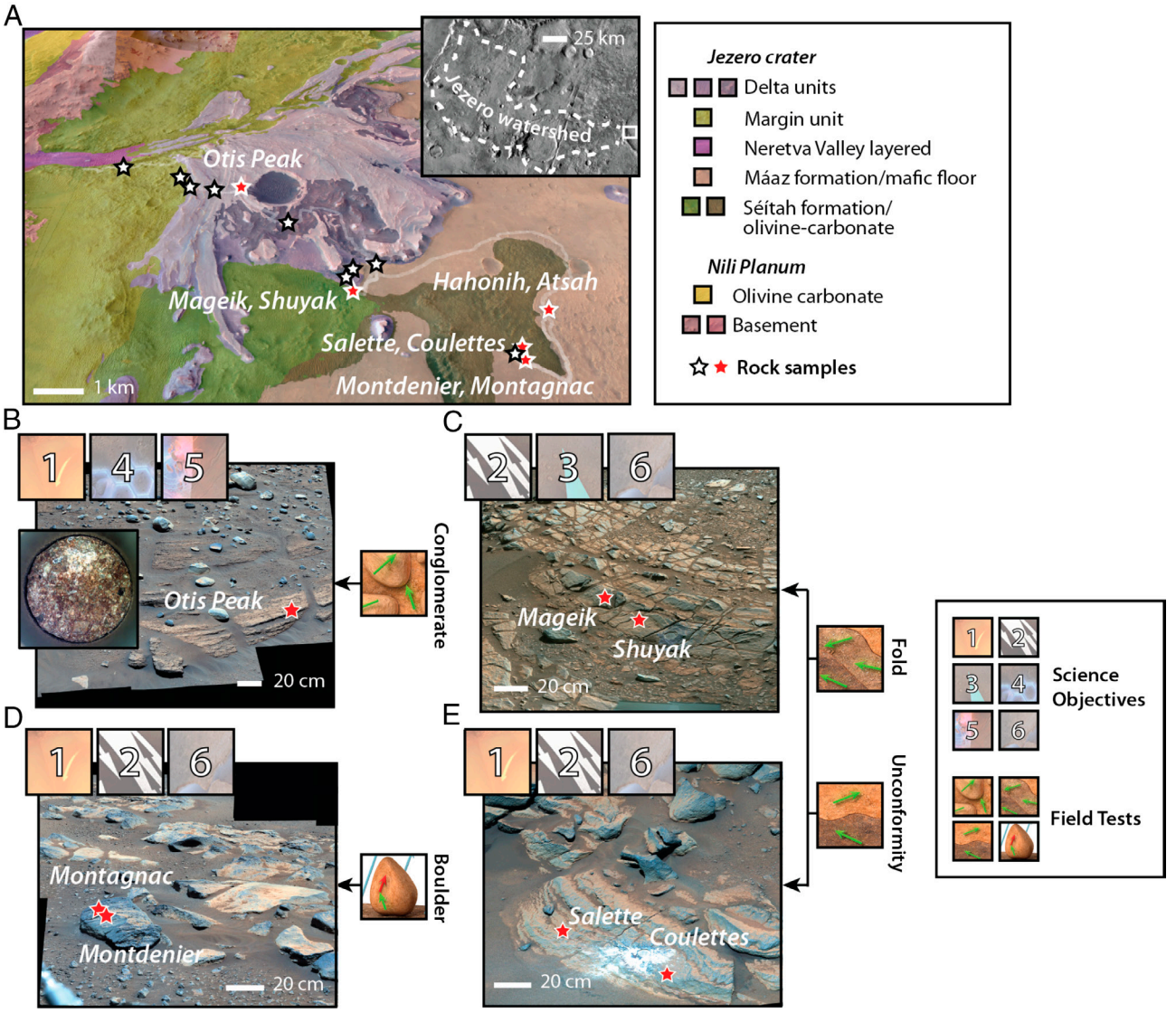

Fig. 4. Mars 2020 and opportunities for magnetic studies of returned samples. (*A*) Shaded relief map geologic map (65) of Jezero crater, draped on High-Resolution Imaging Experiment (HiRISE) (66) images and a HiRISE stereophotogrammetry digital elevation model. White trace shows rover traverse up to sol 1145. Geologic units shown in legend at *Right*. Stars denote sampling locations of rock cores up to sol 1145; red stars denote selected samples shown in (*B–E*) and/or mentioned in the main text (Hahonih and Atsah). (*B*) Delta bedrock conglomerate sampling location of Otis Peak core. Part of Mastcam-Z (67, 68) right eye sol 821 imaging sequence zcam08838, displayed in enhanced RGB color. The inset shows an enhanced color version of a sol 822 CacheCam image (68) from sequence cach00227 of core bottom. (*C*) Delta sandstone bedrock sampling locations of Mageik and Shuyak cores. Part of Mastcam-Z left eye sol 569 sequence zcam08590, displayed in enhanced RGB color. (*D*) Máaz boulder sampled by Montdenier and Montagnac cores. Part of Mastcam-Z left eye sol 180 sequence zcam08195, displayed in enhanced RGB color. (*E*) Séítah bedrock sampled by Salette and Coulettes cores. Part of Mastcam-Z left eye sol 255 sequence zcam08283, displayed in enhanced RGB color. Boxed numbers indicate science objectives (Fig. 1) potentially addressable with samples. Boxes at *Right* in *B–E* denote field tests (Fig. 2) that could be conducted at each location.

A regional scale fold test comparing the samples from the tilted crater floor (e.g., the Salette, Coulettes, Hahonih, and Atsah cores) to those from the flat-lying delta (e.g., the Otis Peak, Mageik, and Shuyak cores) could establish that the magnetization predates tilting (Figs. 2 *C* and *D* and 4 *B*, *C*, and *E*). Comparisons of the VRM overprints from Máaz cores acquired from a boulder (the Montdenier and Montagnac cores) with those from the bedrock (the Hahonih and Atsah cores) could establish that the stable NRM is from a dynamo rather than the local crustal field (e.g., Figs. 2 *G* and *H* and 4*D*) (*Objective 1*) and measure the intensity of the present-day crustal field (*Objective 5*).

All bedrock samples should provide paleodirectional measurements that can constrain the dynamo geometry and search for evidence of polar wander (*Objectives 2 and 3*). Coupled magnetic and petrologic studies of different mineral assemblages and clasts will be valuable for understanding the likelihood that early formed biosignatures have been preserved (*Objective 4*). Analyses of aqueously altered sedimentary (e.g., the Mageik and Shuyak cores) and igneous rocks (e.g., the Salette and Coulettes cores) can test the hypothesis that the strong crustal anomalies reflect CRM carried by authigenic magnetite (*Objective 5*). Conglomerate tests (Figs. 2 *A* and *B* and 4*B*) on the fan pebble conglomerate samples (e.g., Otis Peak core) could establish whether the alteration minerals within the clasts formed after deposition in Jezero or were allochthonously transported into the crater from Nili Planum (*Objective 6*). Paleodirectional data could be used to identify hiatuses and unconformities including bedding-parallel structures that may be invisible in rover images (Figs. 2 *E* and *F* and 4 *C* and *E*). Conversely, an unconformity test (Figs. 2 *E* and *F* and 4 *C* and *E*) across the Séítah-basal delta unconformity (e.g., using the Salette, Coulettes, Mageik, and

Shuyak cores) could establish an ancient age for the magnetization in the delta rocks. Rock magnetic constraints will also constrain the redox state of the igneous and sedimentary environments in which the samples formed and were later altered (*Objective 6*).

Implications for Future Sampling and the MSR Campaign. As discussed in *SI Appendix, Text*, to ensure that we can study magnetization in bedrock formed during the lifetime of the dynamo, we recommend Mars 2020 acquire future samples from layered Nili Planum basement lithologies and megabreccia blocks outside Jezero crater. Given that future MSR paleomagnetic studies will be strongly limited by the smaller number of samples relative to those used for typical Earth studies (*Introduction to Paleomagnetism and Rock Magnetism*), we advocate maximizing the number of returned samples be returned to Earth [e.g., ideally reaching 30; (2)]. We also describe in *SI Appendix, Text* how the above paleomagnetic studies rely on the downstream MSR missions and curation adequately maintaining the samples' NRMs and orientation information. In particular, the samples should not be exposed to temperatures above 60 °C or fields >0.5 mT following sampling, and the orientation and magnetization of each core should be documented soon after opening the sample tubes on Earth and prior to subdividing them.

Summary

The history of the ancient Martian magnetic field likely had major implications for the evolution of the atmosphere and the habitability of Mars. However, there have been no unambiguous measurements of the strength or direction of the dynamo field from either laboratory measurements of Martian meteorites or spacecraft observations of the Martian crust. Future measurements of returned samples being acquired by the Perseverance rover should enable the first direct measurements of the intensity of the Martian dynamo field and constrain its time of onset and termination. As the first absolutely oriented, stratigraphically bound bedrock sample suite from another solar system body, laboratory measurements will also enable the first measurements of the paleodirection of a planetary magnetic field. These measurements will also constrain the relative timing and preservation state of potential biosignatures in the samples and enable tests of the hypotheses that Mars experienced plate tectonics and/or true polar wander. To ensure that we acquire the earliest bedrock records of Martian magnetism, Perseverance should target layered basement and megabreccia outside the crater for future sampling. Finally, to ensure the success of these objectives, downstream MSR missions and sample curation should avoid remagnetizing the samples and should document their orientations.

Data, Materials, and Software Availability. All study data are included in the article and/or *SI Appendix*.

ACKNOWLEDGMENTS. We thank Hap McSween and Mark Thiemens for organizing this volume and Bruce Banerdt and an anonymous reviewer for helpful reviews. We also thank the Mars 2020 and MSR Campaign scientists and engineers. We thank Hernán Cañellas for drafting images for Figs. 1 and 2. B.P.W. also thanks A. Muxworthy, J. Feinberg, J. Gattacceca, and J. Kirschvink for helpful conversations. B.P.W. and E.N.M. thank the NASA Mars 2020 Returned Sample Science Participating Scientist program (grant 80NSSC20K0238), C.M. thanks the Centre National D'Etudes Spatiales (CNES for funding, and C.J.S. acknowledges support from the NSF (awards 2016763, 2054605, 2237807, 2321344, and 2245629).

1. A. Mittelholz, C. L. Johnson, The Martian crustal magnetic field. *Front. Astron. Space Sci.* **9**, 895362 (2022).
2. M. A. Meyer *et al.*, Final report of the Mars sample return science planning group 2 (MSPG2). *Astrobiology* **22**, S5–S26 (2022).
3. D. W. Beaty *et al.*, The potential science and engineering value of samples delivered to Earth by Mars sample return. *Meteorit. Planet. Sci.* **54**, 667–671 (2019).
4. A. Mittelholz *et al.*, The Mars 2020 candidate landing sites: A magnetic field perspective. *Earth Space Sci.* **5**, 410–424 (2018).
5. D. J. Dunlop, O. Özdemir, *Rock Magnetism: Fundamentals and Frontiers* (Cambridge University Press, New York, 1997), p. 573.
6. M. T. Merrill, M. W. McElhinny, P. L. McFadden, *The Magnetic Field of the Earth: Paleomagnetism, the Core, and the Deep Mantle* (Academic Press, San Diego, ed. 2, 1998), p. 531.
7. J. L. Kirschvink, The Precambrian-Cambrian Boundary Problem: Paleomagnetic directions from the Amadeus Basin, Central Australia. *Earth Planet. Sci. Lett.* **40**, 91–100 (1978).
8. L. Tauxe, *Essentials of Paleomagnetism* (Fifth Web Edition, University of California Press, 2018).
9. T. D. Raub, J. L. Kirschvink, D. A. D. Evans, "True polar wander: Linking deep and shallow geodynamics to hydro- and bio-spheric hypotheses" in *Treatise on Geophysics*, M. Kono, Ed. (Elsevier, 2007), pp. 565–589.
10. A. Du *et al.*, Ground magnetic survey on Mars from the Zhurong rover. *Nature Astron.* **7**, 1037–1047 (2023).
11. M. B. Madsen *et al.*, Overview of the magnetic properties experiments on the Mars Exploration Rovers. *J. Geophys. Res.* **114**, E06S90 (2009).
12. T. F. Bristow *et al.*, The origin and implications of clay minerals from Yellowknife Bay, Gale crater, Mars. *Am. Miner.* **100**, 824–836 (2015).
13. B. Langlais, E. Thébault, A. Houliez, M. E. Purucker, R. J. Lillis, A new model of the crustal magnetic field of Mars using MGS and MAVEN. *J. Geophys. Res.* **124**, 1542–1569 (2019).
14. R. Wordsworth, The climate of early Mars. *Annu. Rev. Earth Planet. Sci.* **216**, 381–408 (2016).
15. A. Mittelholz, C. L. Johnson, J. M. Feinberg, B. Langlais, R. J. Phillips, Timing of the martian dynamo: New constraints for a core field 4.5 and 3.7 Ga ago. *Sci. Adv.* **6**, eaba0513 (2020).
16. S. Marchi, A new Martian crater chronology: Implications for Jezero crater. *Astronom. J.* **161**, 187 (2021).
17. W. F. Bottke, J. C. Andrews-Hanna, A post-accretionary lull in large impacts on early Mars. *Nature Geosci.* **10**, 344–348 (2017).
18. F. Vervelidou, V. Lesur, M. Grott, A. Morschhauser, R. J. Lillis, Constraining the date of the Martian dynamo shutdown by means of crater magnetization signatures. *J. Geophys. Res.* **122**, 2294–2311 (2017), 10.1002/2017JE005410.
19. B. Langlais, M. Purucker, A polar magnetic paleopole associated with Apollinaris Patera, Mars. *Planet. Space Sci.* **55**, 270–279 (2007).
20. C. Milbury, G. Schubert, C. A. Raymond, S. E. Smrekar, B. Langlais, The history of Mars' dynamo as revealed by modeling magnetic anomalies near Tyrrhenus Mons and Syrtis Major. *J. Geophys. Res.* **117**, E10007 (2012).
21. K. M. Stack *et al.*, Sedimentology and stratigraphy of the Shenandoah formation, western fan, Jezero Crater, Mars. *J. Geophys. Res.* **129**, e2023JE008187 (2024).
22. B. Horgan *et al.*, Mineralogy, morphology, and emplacement history of the Maaz formation on the Jezero crater floor from orbital and rover observations. *J. Geophys. Res.* **128**, e2022JE007612 (2023).
23. L. Mandon *et al.*, Refining the age, emplacement and alteration scenarios of the olivine-rich unit in the Nili Fossae region, Mars. *Icarus* **336**, 113436 (2020).
24. E. L. Scheller, B. L. Ehlmann, Composition, stratigraphy, and geological history of the Noachian Basement surrounding the Isidis impact basin. *J. Geophys. Res.* **125**, e2019JE006190 (2020).
25. G. G. Michael, Planetary surface dating from crater size–frequency distribution measurements: Multiple resurfacing episodes and differential isochron fitting. *Icarus* **226**, 885–890 (2013).
26. G. Schubert, C. T. Russell, W. B. Moore, Timing of the Martian dynamo. *Nature* **408**, 666–667 (2000).
27. A. Mittelholz *et al.*, Magnetic field signatures of craters on Mars. *Geophys. Res. Lett.* **51**, e2023GL106788 (2024).
28. S. C. Steele *et al.*, Weak magnetism of Martian impact basins may reflect cooling in a reversing dynamo. *Nat. Commun.* **15**, 6831 (2024).
29. S. L. Murchie *et al.*, A synthesis of Martian aqueous mineralogy after 1 Mars year of observations from the Mars Reconnaissance Orbiter. *J. Geophys. Res.* **114**, E00D06 (2009), 10.1029/2009JE003342.
30. A. H. Treiman *et al.*, Mineralogy, provenance, and diagenesis of a potassic basaltic sandstone on Mars: CheMin X-ray diffraction of the Windjana sample (Kimberley area, Gale Crater). *J. Geophys. Res.* **121**, 75–106 (2016).
31. A. Udry *et al.*, What Martian meteorites reveal about the interior and surface of Mars. *J. Geophys. Res.* **125**, e2020JE006523 (2020).
32. The Meteoritical Society,Meteoritical bulletin database. https://www.lpi.usra.edu/meteor/. Accessed 10 May 2024.
33. J. Gattacceca *et al.*, Opaque minerals, magnetic properties, and paleomagnetism of the Tissint Martian meteorite. *Meteorit. Planet. Sci.* **48**, 1919–1936 (2013).
34. F. Vervelidou, B. P. Weiss, F. Lagroix, Hand magnets and the destruction of ancient meteorite magnetism. *J. Geophys. Res.* **128**, e2022JE007464 (2023).
35. S. C. Steele *et al.*, Paleomagnetic evidence for a long-lived, potentially reversing martian dynamo at ~3.9 Ga. *Sci. Adv.* **9**, eade9071 (2023).
36. B. P. Weiss, L. E. Fong, H. Vali, E. A. Lima, F. Baudenbacher, Paleointensity of the ancient Martian magnetic field. *Geophys. Res. Lett.* **35**, L23207 (2008), 10.1029/2008GL035585.
37. J. Gattacceca *et al.*, Martian meteorites and Martian magnetic anomalies: A new perspective from NWA 7034. *Geophys. Res. Lett.* **41**, 4859–4864 (2014).
38. C. D. K. Herd *et al.*, The Northwest Africa 8159 martian meteorite: Expanding the martian sample suite to the early Amazonian. *Geochim. Cosmochim. Acta* **218**, 1–26 (2017).
39. R. L. Parker, A theory of ideal bodies for seamount magnetism. *J. Geophys. Res.* **96**, 16101–16112 (1991).
40. B. P. Weiss, J. Gattacceca, S. Stanley, P. Rochette, U. R. Christensen, Paleomagnetic records of meteorites and early planetesimal differentiation. *Space Sci. Rev.***152**, 341–390 (2009).

41. B. P. Weiss *et al.*, Oriented bedrock samples drilled by the Perseverance rover on Mars. *Earth Space Sci.* **11**, e2023EA003322 (2024).
42. R. Y. Sheppard, M. E. Thorpe, A. A. Fraeman, V. K. Fox, R. E. Milliken, Merging perspectives on secondary minerals on Mars: A review of ancient water-rock interactions in Gale crater inferred from orbital and in-situ observations. *Minerals* **11**, 986 (2021).
43. B. M. Jakosky *et al.*, Loss of the Martian atmosphere to space: Present-day loss rates determined from MAVEN observations and integrated loss through time. *Icarus* **315**, 146–157 (2018).
44. H. Gunell *et al.*, Why an intrinsic magnetic field does not protect a planet against atmospheric escape. *Astron. Astrophys.* **614**, L3 (2018).
45. D. Hemingway, P. E. Driscoll, History and future of the Martian dynamo and implications of a hypothetical solid inner core. *J. Geophys. Res.* **126**, e2020JE006663 (2021).
46. F. Nimmo, D. Stevenson, Influence of early plate tectonics on the thermal evolution and magnetic field of Mars. *J. Geophys. Res.* **105**, 11969–11979 (2000).
47. U. R. Christensen, Dynamo scaling laws and applications to the planets. *Space Sci. Rev.* **152**, 565–590 (2010).
48. P. Olson, H. Amit, Magnetic reversal frequency scaling in dynamos with thermochemical convection. *Phys. Earth Planet. Inter.* **229**, 122–133 (2014).
49. D. Breuer, T. Spohn, Early plate tectonics versus single-plate tectonics on Mars: Evidence from magnetic field history and crust evolution. *J. Geophys. Res.* **108**, 5072 (2003).
50. J. E. P. Connerney *et al.*, Tectonic implications of Mars crustal magnetism. *Proc. Natl. Acad. Sci. U.S.A.* **102**, 14970–14975 (2005).
51. H. J. Melosh, Tectonic patterns on a reoriented planet: Mars. *Icarus* **44**, 745–751 (1980).
52. S. Bouley *et al.*, Late Tharsis formation and implications for early Mars. *Nature* **531**, 334–337 (2016).
53. E. S. Kite, I. Matsuyama, M. Manga, J. T. Perron, J. X. Mitrovica, True Polar Wander driven by late-stage volcanism and the distribution of paleopolar deposits on Mars. *Earth Planet. Sci. Lett.* **280**, 254–267 (2009).
54. P. Thomas, M. Grott, A. Morschhauser, F. Vervelidou, Paleopole reconstruction of Martian magnetic field anomalies. *J. Geophys. Res.* **123**, 1140–1155 (2018).
55. J. T. Perron, J. X. Mitrovica, M. Manga, I. Matsuyama, M. A. Richards, Evidence for an ancient martian ocean in the topography of deformed shorelines. *Nature* **447**, 840–843 (2007).
56. E. R. D. Scott, M. Fuller, A possible source for the Martian crustal magnetic field. *Earth Planet. Sci. Lett.* **220**, 83–90 (2004).
57. Y. Quesnel *et al.*, Serpentinization of the martian crust during Noachian. *Earth Planet. Sci. Lett.* **277**, 184–193 (2009).
58. B. P. Weiss, Y. L. Yung, K. H. Nealson, Atmospheric energy for subsurface life on Mars? *Proc. Natl. Acad. Sci. U.S.A.* **97**, 1395–1399 (2000).
59. N. J. Tosca, I. A. M. Ahmed, B. M. Tutolo, A. Ashpitel, J. A. Hurowitz, Magnetite authigenesis and the warming of early Mars. *Nat. Geosci.* **11**, 635–639 (2018).
60. D. H. Tarling, F. Hrouda, *The Magnetic Anisotropy of Rocks* (Chapman & Hall, London, 1993), p. 217.
61. S. P. Slotznick *et al.*, Reconstructing the paleoenvironment of an oxygenated Mesoproterozoic shoreline and its record of life. *Geol. Soc. Am. Bull.* **136**, 1628–1650 (2023).
62. T. Berndt, A. R. Muxworthy, Dating Icelandic glacial floods using a new viscous remanent magnetization protocol. *Geology* **45**, 339–342 (2017).
63. G. A. Paterson *et al.*, Paleomagnetic determination of emplacement temperatures of pyroclastic deposits: An under-utilized tool. *Bull. Volcanol.* **72**, 309–330 (2010).
64. S. Holm-Alwmark *et al.*, Stratigraphic relationships in Jezero crater, Mars: Constraints on the timing of fluvial-lacustrine activity from orbital observations. *J. Geophys. Res.* **126**, 113436 (2021).
65. K. M. Stack *et al.*, Photogeologic map of the perseverance rover field site in Jezero Crater constructed by the Mars 2020 Science Team. *Space Sci. Rev.* **216**, 1–47 (2020).
66. A. S. McEwen *et al.*, Mars reconnaissance orbiter's high resolution imaging science experiment (HiRISE). *J. Geophys. Res.* **112**, E05S02 (2007), 10.1029/2005JE002605.
67. J. F. Bell *et al.*, The Mars 2020 Perseverancer rover Mast Camera Zoom (Mastcam-Z) multispectral, stereoscopic imaging investigation. *Space Sci. Rev.* **217**, 24 (2021).
68. NASA/JPL, Mars Perseverance Raw Images. https://mars.nasa.gov/mars2020/multimedia/raw-images. Accessed 10 May 2024.
69. N. Mangold *et al.*, Perseverance rover reveals an ancient delta-lake system and flood deposits at Jezero crater, Mars. *Science* **374**, 711–717 (2021).
70. K. A. Farley, K. M. Stack, Mars 2020 initial ereports: Volume 1. Crater Floor Campaign. http://doi.org/10.17189/68tf-re13.
71. K. A. Farley, K. M. Stack, Mars 2020 initial reports: Volume 2. Delta Front Campaign. http://doi.org/10.17189/49zd-2k55.
72. C. D. K. Herd *et al.*, Sampling Mars: Geologic context and preliminary characterization of samples Collected by the NASA Mars 2020 Perseverance rover mission. *Proc. Natl. Acad. Sci. U.S.A.*, this issue (2024).
73. J. I. Simon *et al.*, Samples collected from the floor of Jezero crater with the Mars 2020 Perseverance rover. *J. Geophys. Res.* **128**, e2022JE007474 (2023).
74. T. Bosak *et al.*, Astrobiological potential of rocks acquired by the Perseverance rover at a sedimentary fan front in Jezero crater, Mars. *AGU Adv.*, **5**, e2024AV001241, 10.1029/2024AV001241 (2024).
75. E. N. Mansbach *et al.*, Likely ferromagnetic minerals identified by the Perseverance rover and implications for future paleomagnetic analyses of returned Martian samples. *J. Geophys. Res.*, 10.1029/2024JE008505 (2024).